

From Pixels to Factors: Learning Independently Controllable State Variables for Reinforcement Learning

Rafael Rodriguez-Sanchez
Brown University
rrs@brown.edu

Cameron Allen
UC Berkeley
camallen@berkeley.edu

George Konidaris
Brown University
gdk@cs.brown.edu

Abstract

Algorithms that exploit *factored* Markov decision processes are far more sample-efficient than factor-agnostic methods, yet they assume a factored representation is known *a priori*—a requirement that breaks down when the agent sees only high-dimensional observations. Conversely, deep reinforcement learning handles such inputs but cannot benefit from factored structure. We address this representation problem with Action-Controllable Factorization (ACF), a contrastive learning approach that uncovers *independently controllable* latent variables—state components each action can influence separately. ACF leverages sparsity: actions typically affect only a subset of variables, while the rest evolve under the environment’s dynamics, yielding informative data for contrastive training. ACF recovers the ground-truth controllable factors directly from pixel observations on three benchmarks with known factored structure—TAXI, FOURROOMS, and MINIGRID-DOORKEY—consistently outperforming baseline disentanglement algorithms.

1 Introduction

Over the last decade, deep reinforcement learning (RL) has enabled agents to learn complex behaviors directly from high-dimensional observations—e.g., pixels in Atari games (Mnih et al., 2015), and continuous control from pixels (Lillicrap et al., 2016; Levine et al., 2016)—without manual feature engineering. However, this flexibility comes at a cost: modern deep RL methods remain strikingly sample-inefficient.

Classical work in factored RL shows that, if the underlying Markov decision process (MDP) can be decomposed into state-variable factors with sparse dependencies, one can achieve exponential gains in both model learning and planning (Boutilier et al., 1995; Guestrin et al., 2003). Indeed, factored variants of PAC-RL algorithms such as factored E^3 (Kearns & Koller, 1999) and Factored RMax (Guestrin et al., 2002; Brafman & Tennenholtz, 2002), provably exploit these structures for faster convergence, and subsequent methods even learn the dependency graph online (Strehl et al., 2007; Diuk et al., 2009). More recently, factored representations have proven useful for world modeling (Wang et al., 2022b; Pitis et al., 2020, 2022), exploration (Wang et al., 2023; Seitzer et al., 2021), and skill discovery (Vigorito & Barto, 2010; Wang et al., 2024; Chuck et al., 2024, 2025). Crucially, all these gains depend on having access to a hand-specified factored representation.

State-of-the-art model-based deep RL approaches avoid simulating trajectories in raw observations by learning latent world models end-to-end (Hafner et al., 2019; Schrittwieser et al., 2020; Hansen et al., 2022; Rodriguez-Sanchez & Konidaris, 2024). Some efforts attempt to induce factorization in these latent spaces (Hansen et al., 2022; Hafner et al., 2025), but they do not offer empirical or theoretical guarantee that any factor is identified. In parallel, unsupervised and self-supervised

learning has long studied disentanglement (Bengio et al., 2013; Locatello et al., 2019) as a way to achieve better generalization. Although there is no consensus formalization of disentanglement, two classical approaches are nonlinear ICA (Independent Component Analysis; Comon (1994); Hyvärinen et al. (2023)) and causal representation learning (Schölkopf et al., 2021) yet these methods do not fully ground to decision making and control. For instance, some methods pretrain disentangled representations for RL (Higgins et al., 2017a) based on the assumption that the learned variables will be useful for downstream decision-making. Meanwhile, causal representation learning (Schölkopf et al., 2021) leverages the notion of interventions, related to an RL agent actions, but do not directly address the sequential decision making problem.

We address this representation gap for factored RL by explicitly targeting the recovery of independently controllable variables (Thomas et al., 2018). Our key idea is to use a contrastive objective that compares the predicted next-state distributions under agent actions against those under the environment’s natural dynamics. Thus, we align our latent factors with the underlying state variables that are controlled independently. We validate our approach on pixel-based versions of Taxi (Dietterich, 2000), MiniGrid-DoorKey (Chevalier-Boisvert et al., 2023; Pignatelli et al., 2024), and FourRooms (Sutton et al., 1999), showing that we can automatically recover controllable state variables that align with an expert-designed representation, directly from the pixels.

Contributions First, we formalize the representation learning problem for factored RL as the problem of identifying *independently controllable* latent variables. Moreover, we propose a novel contrastive learning objective that leverages action-induced discrepancies in next-state predictions to isolate controllable factors. Finally, we demonstrate empirically that our method recovers ground-truth controllable factors directly from pixels in classical RL domains.

2 Background

Markov Decision Process We consider an agent that acts in a Markov Decision Process (MDP; Puterman (1994)) $\mathcal{M} = \langle \mathcal{S}, A, T, R, p_0, \gamma \rangle$ with a continuous state space $\mathcal{S} \subseteq \mathbb{R}^{d_s}$ and a discrete action set A . The transition function $T : \mathcal{S} \times A \rightarrow \Delta(\mathcal{S})$ ¹ models the world’s dynamics, $R : \mathcal{S} \times A \rightarrow \mathbb{R}$ is a reward function, $\gamma \in [0, 1)$ is the discount factor, and $p_0 \in \Delta(\mathcal{S})$ is the initial state distribution.

Factored MDPs (FMDPs; Boutilier & Dearden (1996)) are a particular class of MDPs that have a factorized transition function:

$$T(s' | s, a) = \prod_{i=1}^K T_i(s'_i | \text{pa}(s'_i), a),$$

where the state space is $\mathcal{S} = \mathcal{S}_1 \times \dots \times \mathcal{S}_K$ and each $\mathcal{S}_i \subseteq \mathbb{R}$. Moreover, $\text{pa}(s'_i) : \mathcal{S}_i \rightarrow \mathcal{P}([K])$, where $\mathcal{P}([K])$ is the power set of $[1, 2, \dots, K]$, and it represents the set of factors required to predict s'_i . Typically, this structure is represented by a Dynamic Bayesian Network (DBN; Boutilier et al. (1995, 2000)).

Nonlinear Independent Component Analysis (ICA; Comon (1994)) is the problem of identifying a set of independent signal sources from entangled measurements. Formally, given a set of generating sources $\{s_i \in \mathcal{S}_i\}_{i=1}^K$ that are independent and distributed according to densities $p(s_i)$, ICA identifies the set of generating signals from observed measurements x that are entangled (mixed) by an unknown function o —i.e., $x = o(s_1, \dots, s_K)$. In the case of non-linear ICA, o is a nonlinear, invertible function. In particular, we will consider the problem of non-linear ICA with auxiliary variables (Hyvärinen et al., 2019), where the sources to be identified are *conditionally* independent given an auxiliary variable u . Moreover, we assume that our agent receives high-dimensional observations that are generated by an observation function that is a diffeomorphism² $o : \mathcal{S} \rightarrow X \subseteq \mathbb{R}^{d_x}$, where $d_x \gg d_s$.

3 ACF: Action Controllable Factorization

Imagine a simple desk lamp with two separate switches: one toggles the lamp’s power, flipping it on or off, while the other cycles the bulb’s color between warm and cold light. If you leave

¹ $\Delta(X)$ is the set of probability densities over set X .

²A bijection that is continuously differentiable and whose inverse is also continuously differentiable.

both switches untouched, the lamp may still occasionally flicker on or change color on its own, but with a significantly lower probability. By observing the lamp when you flip only the power switch versus doing nothing, you isolate the “on/off” factor; likewise, by pressing only the color switch versus leaving it alone, you isolate the “color” factor. Because each switch only affects one property while the other property evolves naturally, you can disentangle these two characteristics simply by contrasting action-driven changes with natural behavior. The lamp might have other characteristics like volume, weight, and shape; however, these are not factors that can be controlled by the agent. Here we focus on disentangling factors that *are* controllable.

3.1 Problem Formulation

Setting We consider that the agent does not have access to the ground truth factored state space S . Instead, it gets high-dimensional observations that are generated by an unknown diffeomorphism $o : S \rightarrow X \subseteq \mathbb{R}^{d_x}$. Hence, we are concerned with learning from the observed samples of $T(x' | x, a)$ an encoder $f_\phi : X \rightarrow Z$, where Z factorizes as $Z = Z_1 \times \dots \times Z_K$, that *identifies* the underlying factors.

Identification Formally, we say that a learned factorization identifies the underlying factor S_i if and only if there exist invertible functions h_i and permutation function ρ such that $h_i : Z_i \rightarrow S_{\rho(i)}$ for all $i \in \{1, \dots, K\}$. That is, we can recover the underlying factors up to permutation and invertible transformations.

In many problems, the agent’s actions have sparse effects on the environment: just a few factors are controlled, while others just follow their natural transition, unaffected by the agent. To help the agent understand its environment, we assume that the agent has a *special action* a_0 that corresponds to a *no-op* (or observe) action that allows the agent to observe the natural evolution of the environment without intervening.

Transition Dynamics Let $\Psi : S \times A \rightarrow \mathcal{P}([1, 2, \dots, K])$ be the set of variables affected by action a in state s . We assume the transition dynamics factorize as follows,

$$T(s' | s, a) = \prod_{i \in \Psi(s, a)} T(s'_i | s, a) \prod_{j \notin \Psi(s, a)} T(s'_j | s, a_0); \quad (1)$$

where $T(s'_i | s, a_0)$ represents the natural (or observational) dynamics. In here, we will consider conditioning the transition dynamics on the full current state s , instead of just the parents, given that $T(s'_i | s, a) = T(s'_i | \text{pa}(s'_i), a)$.

Moreover, for the unknown observation function o , a diffeomorphism, we know that the *observed* dynamics follow (Boothby, 2003):

$$T(x' | x, a) = |\det(J_{o^{-1}}(x')^T J_{o^{-1}}(x))|^{1/2} T(s' | s, a), \quad (2)$$

This equation relates the observed dynamics $T(x' | x, a)$ to the underlying ground truth state dynamics $T(s' | s, a)$ by the Jacobian matrix $J_{o^{-1}}$, whose determinant quantifies the change in volume between the two spaces. This relation can be seen as the generalization to higher dimensions of the change of variable formula in probability theory.

3.2 Algorithm

Energy Parameterization We parameterize the encoder by $f_\phi(x) \mapsto z$, with parameters ϕ , and, more importantly, we parameterize the transition function as the sum of energy functions (unnormalized probability densities) such that, $T(z' | z, a) \propto \exp\left(\sum_{i=1}^K E_\theta(z'_i, a, z)\right)$ with $i \in [K]$ and parameters θ . This sum of energies reflects the factorized structure where each energy represent the transition dynamics of latent variable z_i .

Learning a Markov Representation In order to estimate these energy functions from data and learn a Markov representation suitable for RL (Allen et al., 2021), we optimize the following training objectives. Firstly, we estimate the inverse dynamics I^π using our energy functions, as follows,

$$I^\pi(a | z, z') = \frac{T(z' | z, a) \pi(a | z)}{\sum_{a'} T(z' | z, a') \pi(a' | z)} \propto \frac{\exp(\sum_i E_\theta(z'_i, a, z)) \pi(a | z)}{\sum_{a' \in A} \exp(\sum_i E_\theta(z'_i, a', z)) \pi(a' | z)}; \quad (3)$$

and because our action set is discrete, we can use a softmax multiclass classifier to learn our inverse function by minimizing the cross entropy loss:

$$\mathcal{L}_{\text{inv}}(\phi, \theta) = -\log I^\pi(a \mid z, z'). \quad (4)$$

Secondly, we use InfoNCE (Oord et al., 2018) to maximize the mutual information between z and z' : we use a batch B of $N - 1$ negative samples and 1 positive sample, and minimize the following loss,

$$\mathcal{L}_{\text{fwd}}(\phi, \theta) = -\log \frac{\exp(\sum_i E_\theta(z'_i, a, z))}{\sum_{z^j \in B} \exp(\sum_i E_\theta(z'_i, a, z))}. \quad (5)$$

Optimizing these losses guarantee that we learn a Markov representation that preserves the relevant information for action effects prediction (Allen et al., 2021) without requiring an explicit reconstruction loss. However, they do not ensure that the representation will align with the controllable factors.

To see this, consider an invertible mapping $g : S \rightarrow Z$ between the ground truth state s and another representation z . The relation between the densities is given by the following change of variable formula: $T(s' \mid s, a) = |\det J_g(s')| T(z' \mid z, a)$. Therefore, if $|\det J_g(s')| = 1$ (e.g., g is a rotation), the distribution will match even in the case we use a factorized prior (for an extended discussion, see Locatello et al. (2019); Hyvärinen et al. (2023))

Factorizing the Controllable Variables We formalize our intuition and exploit the sparsity of the actions' effects to learn a latent representation Z that identifies the controllable factors.

The core idea is to contrast the effect of an action, the distribution $T(x' \mid x, a)$, against the natural dynamics $T(x' \mid x, a_0)$, where a_0 is the no-op action, using the following ratio:

$$\begin{aligned} \log r_a(x', x) &= \log \frac{T(x' \mid x, a)}{T(x' \mid x, a_0)} = \log \frac{|\det(J_{o-1}(x')^T J_{o-1}(x'))|^{1/2} \prod_i T(s'_i \mid s, a)}{|\det(J_{o-1}(x')^T J_{o-1}(x'))|^{1/2} \prod_i T(s'_i \mid s, a_0)}, \\ &= \log \frac{T(s'_j \mid s, a)}{T(s'_j \mid s, a_0)} = \log r_a(s', s), \end{aligned}$$

where s'_j is the factor affected by a when executed in s . Therefore, this ratio is a function of the factor s'_j and not the rest.

In practice, we can estimate these ratios from observed transitions contrastively (Gutmann & Hyvärinen, 2010; Hyvärinen et al., 2019). We leverage our energy parameterization to infer a binary classifier that differentiate between transitions from action a from another, e.g. the null action a_0 .

These classifiers can be computed from the energies using a sigmoid function σ :

$$\sigma(\log r_a(z', z)) := \sigma(\log r_a(f_\phi(x'), f_\phi(x))) = \sigma \left(\sum_i E_\theta(z'_i, a, z) - E_\theta(z'_i, a_0, z) \right).$$

Finally, we train our energy functions to match the observed ratios by training $|A| - 1$ classifiers computed by $\sigma(\log r_a(z', z))$. We use the transitions of other actions as negative samples and minimize the following binary cross-entropy loss:

$$\mathcal{L}_r(\theta, \phi) = \sum_{a' \in A} [a' = a] \log \sigma(\log r_a + \zeta_a) + [a' \neq a] \log (1 - \sigma(\log r_a + \zeta_a)); \quad (6)$$

where $[\cdot]$ is indicator functions that is 1 when the condition holds, and $\zeta_a := \log \frac{\pi(a|z)}{\pi(a_0|z)}$ are correction weights to account for the policy used to collect the data. In practice, we estimate the policy from the dataset and use the estimate to compute the loss. Finally, we minimize a weighted sum of these losses and use AdamW as our optimizer (Loshchilov & Hutter, 2019). Algorithm 1 formalizes the approach.

Identifiability The core assumption of ACF is that variables are independently controllable, that is, for every state variable s_i , there exists a context $s \in \mathcal{S}$ and action $a \in A$, where the action effect is sufficiently different from the natural dynamics of the variable (a_0 effect). The following theorem establishes identifiability of independently controllable factors if the solution found is sparse.

Algorithm 1 Action Controllable Factorization

Require: Dataset $\mathcal{D} = \{(x, a, x')\}$, encoder f_ϕ , set per-factor energy models $\{E_\theta^k\}_{k=1}^K$, policy π_w , Learning rate α , weights $\beta_r, \beta_{\text{fwd}}, \beta_{\text{inv}}, \beta_\pi$

- 1: **for** minibatch $\{(x^n, a^n, x'^n)\}_{n=1}^N \sim \mathcal{D}$ **do**
- 2: Encode: $z^n \leftarrow f_\phi(x^n), z'^n \leftarrow f_\phi(x'^n)$
- 3: Noise: $z^n \leftarrow z^n + \varepsilon^n, z'^n \leftarrow z'^n + \varepsilon'^n$
- 4: Negatives: $\mathcal{N} = \{(z^i, a^j, z'^j) \mid i, j = 1, \dots, N\}$
- 5: Energies: $E_{ij}(a) = \sum_k E_\theta^k(z'^j, a, z^i) \forall i, j \in [N], k \in [K], a \in A$
- 6: Policy logits: $\pi_{\text{logits}}^n = \pi_w(z^n) \forall n$
 {The diagonal values are the energy that correspond to real transitions}
- 7: Ratios: $\log r_a^{nn} = E_{nn}(a) - E_{nn}(a_0)$
- 8: Policy weights: $\zeta_a^n = \log \frac{\pi(a^n | z^n)}{\pi(a_0 | z^n)}$
- 9: $\mathcal{L}_r = -\frac{1}{N} \sum_n \sum_a [a^n = a] \log \sigma(\log r_a^{nn} + \text{sg}(\zeta_a^n)) +$
 $[a^n \neq a] \log(1 - \sigma(\log r_a^{nn} + \text{sg}(\zeta_a^n)))$
- 10: $\mathcal{L}_{\text{fwd}} = -\frac{1}{N} \sum_n \log \frac{e^{E_{nn}(a^n)}}{\sum_j e^{E_{nj}(a^n)}}$
- 11: $\mathcal{L}_{\text{inv}} = -\frac{1}{N} \sum_n \log \frac{\pi(a^n | z^n) e^{E_{nn}(a^n)}}{\sum_{a'} \pi(a' | z^n) e^{E_{nn}(a')}}$
- 12: $\mathcal{L}_\pi = \frac{1}{N} \sum_n -\log \frac{e^{\pi_{\text{logits}}^n[a^n]}}{\sum_{a'} e^{\pi_{\text{logits}}^n[a']}}$
- 13: $\mathcal{L} = \beta_r \mathcal{L}_r + \beta_{\text{fwd}} \mathcal{L}_{\text{fwd}} + \beta_{\text{inv}} \mathcal{L}_{\text{inv}} + \beta_\pi \mathcal{L}_\pi$
- 14: Update: $(\phi, \theta, w) \leftarrow \text{AdamW}((\phi, \theta, w), \alpha, \nabla \mathcal{L})$
- 15: **end for**

Theorem 3.1 (Identifiability of the Independently Controllable Factors). *Let the learned encoder $f : X \rightarrow Z$ be a diffeomorphism. If the following conditions hold*

1. $\mathcal{S} \subset \mathbb{R}^K$ is connected and the unknown observation function $o : \mathcal{S} \rightarrow X$ is a diffeomorphism.
2. The action effects are **sufficiently different** from the natural dynamics. That is, there exists $i \in [K]$

$$\frac{\partial}{\partial s'_i} \frac{T_i(s'_i | s, a)}{T(s'_i | s, a_0)} \neq 0$$

for $s \in \tilde{\mathcal{S}} \subseteq \mathcal{S}$, almost surely. Moreover, there exists at least an action that affects each s_i (independent controllability)

3. All energy function approximate the factor forward dynamics $E(z'_i, a, z) \propto \log T(z'_i | z, a)$;
4. (**Sparsity**) The score differences (gradients of the energies)

$$\frac{\partial}{\partial z'_i} \Delta E_i^a = \frac{\partial}{\partial z'_i} [E(z'_i, a, z) - E(z'_i, a_0, z)] \neq 0$$

for at most one variable j and all actions.

then, there exists a factor-wise diffeomorphism $h : \mathcal{S} \rightarrow Z$ between the underlying ground truth factors of variation \mathcal{S} and the learned encoding Z

Similar arguments have been used to establish identifiability under action and state-dependency sparsity (Lachapelle et al., 2022, 2024) and under single-node interventions in causal representation learning (Varici et al., 2024). Theorem 3.2 can be viewed as a special case of these results adapted to the independently controllable factors setting³. This result further shows that independently controllable factors can be recovered when, in addition to certain regularity and variability conditions,

³The proof is provided in Appendix A

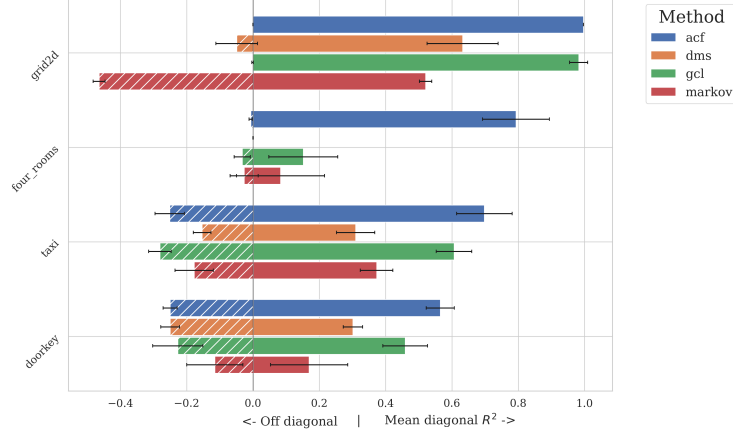


Figure 1: **Factorization metrics.** The left side bars show how much of the information is represented off the diagonal on average over all variables. The right side bars represent the mean diagonal value. Ideally, we would expect our R^2 matrices to be close to the identity: 0 on the left bar, 1 on the right bar. The error bars show the standard deviation over 5 independent seeds.

the solution is sparse (Condition 4). We conjecture that the binary classifiers arising from the \mathcal{L}_r loss promote sparsity by *competing* to capture what makes each action distinct with respect to both the natural dynamics and the other actions—namely, the specific factor influenced by the action. In the next section, we demonstrate empirically that ACF indeed identifies the independently controllable factors in practice.

4 Evaluation

In this section, we empirically evaluate ACF in RL test domains directly from pixel observations. We consider the visual variation of the classical Taxi domain (Dietterich, 2000) and visual Minigrid environments (Chevalier-Boisvert et al., 2023): FourRooms (Sutton et al., 1999) and DoorKey⁴. We chose these domains because they allow easy access to the generating factors for evaluation and while these domains are simple from the perspective of learning a policy, they actually are challenging from the factorization problem perspective, as we will see in the quantitative results.

Baselines We consider GCL (Generalized Contrastive Learning; Hyvärinen et al. (2019)) that can be seen as a vanilla contrastive-based disentanglement algorithm, and DMS (Disentanglement via Mechanism Sparsity; Lachapelle et al. (2022)), a VAE-based (Kingma & Welling, 2014) method that explicitly maximizes sparsity in state dependencies and action effects to drive disentanglement. Moreover, we consider MSA (Markov State Abstractions; Allen et al. (2021)), a contrastive-based algorithm that leverages both forward and inverse dynamics to learn Markovian representations but does not explicitly optimize for disentanglement.

Evaluation Protocol To measure disentanglement, we consider test datasets of pairs of $\{(s^i, z^i)\}_i$ where s is the ground truth representation and z is the corresponding learned latent representation. Then, we fit factor-wise regressors (parameterized by feed-forward networks), $h_{ij}(z_i) \mapsto s_j$. The performance of h_{ij} is limited by the amount of information z_i contains about s_j , therefore we measure the quality of the learned regressor using the coefficient of determination R^2 . Therefore, for each method we have a matrix R^2 (see Figure 2); this matrix would have 1 in the diagonal and low off-diagonal values if the ground truth variables were perfectly identified. We tune all methods via random search in their respective hyperparameter space and train 5 seeds for each method (see Appendix B).

Quantitative results Given a R^2 matrix, we search a permutation that maximizes the diagonal using the Hungarian algorithm (Kuhn, 1955). We then aggregate the matrices into two scores, the mean diagonal value, $\frac{1}{K} \sum_i R_{ii}^2$ and the mean maximum off-diagonal value $\frac{1}{K} \sum_i \max_{j \neq i} R_{ij}^2$. The

⁴We use Minigrid JAX (Bradbury et al., 2018) re-implementation (Pignatelli et al., 2024)

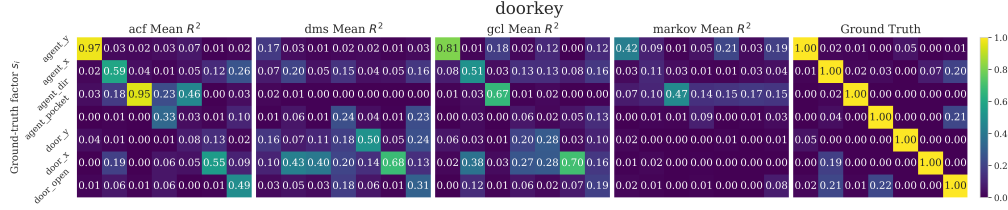


Figure 2: **Factorization matrices for DoorKey.** Mean R^2 matrices over 5 seeds.

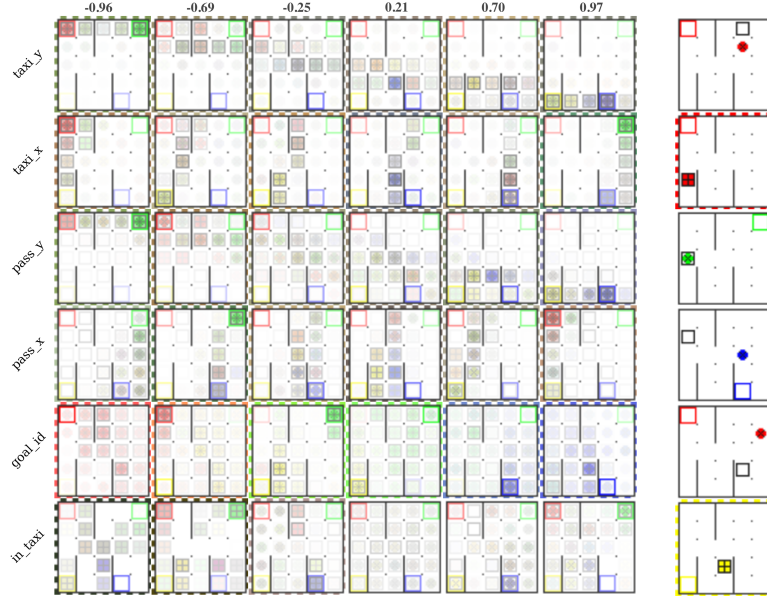


Figure 3: **Taxi latent traversals.** In this Taxi rendering, the taxi is represented by a hollow square, the passengers are circles with colors matching their goal positions. When a passenger is in the taxi, the border of the frame is highlighted with stripes. By varying the value of a latent variable (columns), we can see its effect on the mean observation. Each row represents different latent variables.

former measures how well a latent factor represents the ground truth factor, and the latter measures how much information is contained in the rest of the factors. Ideally, this would mean a score of 1 for the mean diagonal and 0 for the off diagonal if the identification is perfect and the factors are fully independent. However, this is only an upper bound on perfect performance in many environments; e.g. taxi and passenger’s position are not fully independent because the passenger can only move if it moves with the taxi. Figure 1 shows the results for all methods and domains.

The factor affected by an action depends on the current state s . Grid2D and FourRooms have different factorizations: In grid2D the agent can move up, down, left and right and 2 dimensions are enough as controllable factors, but in FourRooms (Minigrid variant) the agent can rotate, move forward, backward, left or right and, hence, 3 factors are required. More importantly, the factor an action affects is *relative to the agent’s orientation* and, this, change causes difficulties for all baseline methods. In particular, DMS, which assumes a global sparse graph, struggles to converge.

Factors are not independent In the Taxi domain, factorization is more challenging because the taxi’s position and the passenger’s location are inherently coupled; the passenger can move only if it moves with the taxi. Our method outperforms the baselines in this case. Figure 3 shows qualitatively the effect of traversing the identified passengers position variables.

Identifying non-controllable variables In the DoorKey domain, not all factors are controllable by the agent: the door’s position is sampled at the start of each episode and kept fixed throughout the episode. Although the agent must perceive the door’s location to open it, that factor need not be disentangled. In fact, as seen in Figure 2, the door y coordinate is not identified. DMS, instead is able

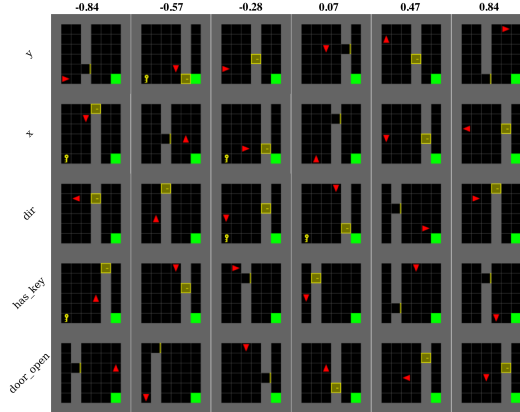


Figure 4: **DoorKey latent traversals.** For this domain, we show a random sample from observations that have a particular value of the latent dimension. We only show the controllable elements in DoorKey, that includes the agent position and orientation, the key and the door state. Different rows correspond to different latent variables and different columns represent different values for the corresponding latent variable.

to partially identify these variables because it’s not constrained to controllable elements and uses the sparsity of the state dependencies.

Ablation We performed an ablation study in the Minigrid-Doorkey domain, the most challenging environment considered in the previous experiments. Table 1 shows that each loss term plays an important role in improving factorization. In addition, we evaluate the *Factored Markov* variant, which combines our unified factored energy parameterization with the MSA losses (forward and inverse). This variant achieves improved factorization compared to the original MSA, highlighting the importance of the our proposed parameterization.

Experiment	Diag Score (Mean \pm Std) \uparrow	Off-Diag Score (Mean \pm Std) \downarrow
ACF (full)	0.5650 \pm 0.0423	0.2499 \pm 0.0213
Factored Markov	0.4861 \pm 0.0491	0.2635 \pm 0.0339
no fwd	0.1987 \pm 0.0588	0.1028 \pm 0.0340
no inv	0.5294 \pm 0.0274	0.1918 \pm 0.0280
no policy	0.4630 \pm 0.0694	0.2301 \pm 0.0543
no ratio	0.5083 \pm 0.0767	0.2353 \pm 0.0352

Table 1: Ablation on Minigrid-Doorkey Enviroment over 5 seeds

5 Related Works

Factored RL There is a long history of leveraging the structure of FMDPs for efficient planning algorithms. By assuming that the structure of the MDP is known (i.e., the DBN), these algorithms exponentially reduce the size of the problem representation. Such algorithms include Structured Value Iteration algorithms (Boutilier & Dearden, 1996; Boutilier et al., 2000) and Structured Policy Iteration (Boutilier et al., 1995; Koller & Parr, 2000), and their extensions to linear approximation (Guestrin et al., 2003). In classical PAC model-based RL algorithms, the Factored E^3 algorithm (Kearns & Koller, 1999) extends the E^3 algorithm (Kearns & Singh, 2002) to the case where the DBN is known and an oracle factored planner is available. Guestrin et al. instantiate this algorithm and RMax Brafman & Tenenholz (2002) using factored linear value iteration (Guestrin et al., 2002) as the planner. Algorithms such as SLF-RMax (Strehl et al., 2007), Met-RMax (Diuk et al., 2009) and SPITI (Degris et al., 2006) loosen the assumption of a known DBN structure and discover this structure online for discrete state spaces. Vigorito & Barto (2009) extends structure learning to continuous state and action spaces. Further theoretical work includes regret bounds for factored RL in the episodic (Osband & Van Roy, 2014; Tian et al., 2020) and non-episodic settings (Xu & Tewari, 2020).

The discovery of the structure among the factored state variables has been used to do exploration (Seitzer et al., 2021; Wang et al., 2023). Closely related, in skill discovery, the factored structure can be exploited to generate signals that facilitate learning useful skills (Vigorito & Barto, 2010; Hu et al., 2024; Wang et al., 2024; Chuck et al., 2024, 2025). Moreover, leveraging the sparsity of edges in the DBN enables algorithms to learn modular world models that are robust (Wang et al., 2022b; Ke et al.). Counterfactual Data Augmentation (CODA) (Pitis et al., 2020, 2022) uses the *local* DBN structure to generate plausible transitions by recombining states based on conditional independence relations that hold locally—i.e., leverages local DBNs to have a nonparametric transition model. However, all of these require knowing the factored representation a priori for these methods to work.

Limited attempts exist to learn factorized representations in deep RL from high-dimensional observations. DARLA (Higgins et al., 2017b) leverages β -VAE representations for zero-shot generalization in multitask RL. Some works that try to learn factored world models include variational causal dynamics models (Lei et al., 2022) and provable factored RL (Misra et al., 2021). DenoisedMDP (Wang et al., 2022a; Liu et al., 2023) factorizes the state in four factors based on their relevance to reward and controllability. TED (Temporal Disentanglement; Dunion et al. (2023)) uses NCE from state transition samples to improve model-free agent robustness to correlated, irrelevant features, and CMID (Conditional Mutual Information for Disentanglement; Dunion et al. (2024)) uses causal, graphical conditions to infer the state factor from pixels. Perhaps, most similar to ours, is the work of Thomas et al. (2018) that proposes to learn independently controllable elements by learning policies that minimize the number of variables changed. However, they obtain limited success in fully aligning a 2D grid learned representation with the ground truth.

Disentanglement in Representation Learning In representation learning (Bengio et al., 2013), disentanglement has been extensively studied (Schmidhuber, 1992; Higgins et al., 2017a; Burgess et al., 2018; Chen et al., 2018; Klindt et al., 2020) as a desirable characteristic for generalizable representations. However, a widely accepted definition of disentanglement does not yet exist and solving this problem without the right inductive biases is impossible (Locatello et al., 2019). Unsupervised approaches leverage the Variational Autoencoder (VAE; Kingma & Welling (2014)) to learn latent representations that have a factorized prior (Kim & Mnih, 2018), minimize total correlation (Chen et al., 2018), and leverage temporal relations (Klindt et al., 2020). An important formalization of disentanglement is Independent Component Analysis (ICA; Comon (1994)). In particular, non-linear ICA (Hyvärinen et al., 2023), where a set of source variables is entangled by an unknown non-linear function. Approaches in non-linear ICA include contrastive methods (Hyvärinen et al., 2019; Hyvärinen & Morioka, 2016), energy functions (Khemakhem et al., 2020b), quantized methods (Hsu et al., 2024a,b), VAEs (Khemakhem et al., 2020a; Klindt et al., 2020) and sparse graphical conditions such as DMS (Disentanglement via Mechanism Sparsity; Lachapelle et al. (2022)). Another approach is causal representation learning (Schölkopf et al., 2021). This tackles the problem of discovering the *causal* variables by leveraging data coming from interventional and observational distributions. In this problem, the variables are not assumed to be independent as in ICA. Simple methods assume having access about what variable was intervened (Lippe et al., 2022, 2023b; Locatello et al., 2020) and assume binary interventions (Lippe et al., 2023a). Recent works establish identifiability results for linear mixing models (Squires et al., 2023), non-linear mixing (Ahuja et al., 2023; Buchholz et al., 2023; Zhang et al., 2023) and non-parametric in the case of unknown interventions (i.e., without labels of the intervened variable) (von Kügelgen et al., 2024; Varici et al., 2024). ACF can be interpreted as a special case where the agent’s actions induce interventional distributions and the natural dynamics are simply the observational distributions.

6 Conclusion

We introduced a new contrastive algorithm for learning a factored representation that recovers the independently controllable variables from high-dimensional observations. We use the fact that RL agents can act upon their environments and create discrepancies in the dynamics; contrasting those controlled dynamics to the natural order of things provides a signal for disentanglement that is relevant for factored RL. Moreover, we showed empirically that our method is able to recover the relevant controllable factors. Nevertheless, not all relevant state variables are necessarily one-step controllable or controllable at all, but we still might be interested in identifying those variables depending on the problem. Therefore, improving agents control over its environment can also serve to further refine factorization and, though out of the scope of this paper, it is an important research direction.

References

- Kartik Ahuja, Divyat Mahajan, Yixin Wang, and Yoshua Bengio. Interventional causal representation learning. In *International conference on machine learning*, pp. 372–407. PMLR, 2023.
- Cameron Allen, Neev Parikh, Omer Gottesman, and George Konidaris. Learning Markov state abstractions for deep reinforcement learning. *Advances in Neural Information Processing Systems*, 34:8229–8241, 2021.
- Yoshua Bengio, Aaron Courville, and Pascal Vincent. Representation learning: A review and new perspectives. *IEEE transactions on pattern analysis and machine intelligence*, 35(8):1798–1828, 2013.
- William M Boothby. *An introduction to differentiable manifolds and Riemannian geometry, Revised*, volume 120. Gulf Professional Publishing, 2003.
- Craig Boutilier and Richard Dearden. Approximate value trees in structured dynamic programming. In *Proceedings of the Thirteenth International Conference on International Conference on Machine Learning*, pp. 54–62, 1996.
- Craig Boutilier, Richard Dearden, Moisés Goldszmidt, et al. Exploiting structure in policy construction. In *IJCAI*, volume 14, pp. 1104–1113, 1995.
- Craig Boutilier, Richard Dearden, and Moisés Goldszmidt. Stochastic dynamic programming with factored representations. *Artificial intelligence*, 121(1-2):49–107, 2000.
- James Bradbury, Roy Frostig, Peter Hawkins, Matthew James Johnson, Chris Leary, Dougal Maclaurin, George Necula, Adam Paszke, Jake VanderPlas, Skye Wanderman-Milne, and Qiao Zhang. JAX: composable transformations of Python+NumPy programs, 2018. URL <http://github.com/jax-ml/jax>.
- Ronen I Brafman and Moshe Tennenholtz. R-max-a general polynomial time algorithm for near-optimal reinforcement learning. *Journal of Machine Learning Research*, 3(Oct):213–231, 2002.
- Simon Buchholz, Goutham Rajendran, Elan Rosenfeld, Bryon Aragam, Bernhard Schölkopf, and Pradeep Ravikumar. Learning linear causal representations from interventions under general nonlinear mixing. *Advances in Neural Information Processing Systems*, 36:45419–45462, 2023.
- Christopher P Burgess, Irina Higgins, Arka Pal, Loic Matthey, Nick Watters, Guillaume Desjardins, and Alexander Lerchner. Understanding disentangling in beta-VAE. *arXiv preprint arXiv:1804.03599*, 2018.
- Ricky TQ Chen, Xuechen Li, Roger B Grosse, and David K Duvenaud. Isolating sources of disentanglement in variational autoencoders. *Advances in neural information processing systems*, 31, 2018.
- Maxime Chevalier-Boisvert, Bolun Dai, Mark Towers, Rodrigo de Lazcano, Lucas Willems, Salem Lahlou, Suman Pal, Pablo Samuel Castro, and Jordan Terry. Minigrid & miniworld: Modular & customizable reinforcement learning environments for goal-oriented tasks. *CoRR*, abs/2306.13831, 2023.
- Caleb Chuck, Kevin Black, Aditya Arjun, Yuke Zhu, and Scott Niekum. Granger causal interaction skill chains. *Transactions on Machine Learning Research*, 2024. ISSN 2835-8856. URL <https://openreview.net/forum?id=iA2KQyoun1>.
- Caleb Chuck, Fan Feng, Carl Qi, Chang Shi, Siddhant Agarwal, Amy Zhang, and Scott Niekum. Null counterfactual factor interactions for goal-conditioned reinforcement learning. In *The Thirteenth International Conference on Learning Representations*, 2025.
- Pierre Comon. Independent component analysis, a new concept? *Signal processing*, 36(3):287–314, 1994.
- Thomas Degris, Olivier Sigaud, and Pierre-Henri Wuillemin. Learning the structure of factored markov decision processes in reinforcement learning problems. In *Proceedings of the 23rd international conference on Machine learning*, pp. 257–264, 2006.

- Thomas G Dietterich. Hierarchical reinforcement learning with the maxq value function decomposition. *Journal of artificial intelligence research*, 13:227–303, 2000.
- Carlos Diuk, Lihong Li, and Bethany R Leffler. The adaptive k-meteorologists problem and its application to structure learning and feature selection in reinforcement learning. In *Proceedings of the 26th Annual International Conference on Machine Learning*, pp. 249–256, 2009.
- Mhairi Dunion, Trevor McInroe, Kevin Sebastian Luck, Josiah P. Hanna, and Stefano V Albrecht. Temporal disentanglement of representations for improved generalisation in reinforcement learning. In *The Eleventh International Conference on Learning Representations*, 2023. URL <https://openreview.net/forum?id=sPgP6aISLTD>.
- Mhairi Dunion, Trevor McInroe, Kevin Sebastian Luck, Josiah Hanna, and Stefano Albrecht. Conditional mutual information for disentangled representations in reinforcement learning. *Advances in Neural Information Processing Systems*, 36, 2024.
- Carlos Guestrin, Relu Patrascu, and Dale Schuurmans. Algorithm-directed exploration for model-based reinforcement learning in factored mdps. In *Proceedings of the Nineteenth International Conference on Machine Learning*, pp. 235–242, 2002.
- Carlos Guestrin, Daphne Koller, Ronald Parr, and Shobha Venkataraman. Efficient solution algorithms for factored mdps. *Journal of Artificial Intelligence Research*, 19:399–468, 2003.
- Michael Gutmann and Aapo Hyvärinen. Noise-contrastive estimation: A new estimation principle for unnormalized statistical models. In Yee Whye Teh and Mike Titterton (eds.), *Proceedings of the Thirteenth International Conference on Artificial Intelligence and Statistics*, volume 9 of *Proceedings of Machine Learning Research*, pp. 297–304, Chia Laguna Resort, Sardinia, Italy, 13–15 May 2010. PMLR.
- Danijar Hafner, Timothy Lillicrap, Ian Fischer, Ruben Villegas, David Ha, Honglak Lee, and James Davidson. Learning latent dynamics for planning from pixels. In *International conference on machine learning*, pp. 2555–2565. PMLR, 2019.
- Danijar Hafner, Jurgis Pasukonis, Jimmy Ba, and Timothy Lillicrap. Mastering diverse control tasks through world models. *Nature*, pp. 1–7, 2025.
- Nicklas A Hansen, Hao Su, and Xiaolong Wang. Temporal difference learning for model predictive control. In *International Conference on Machine Learning*, pp. 8387–8406. PMLR, 2022.
- Jonathan Heek, Anselm Levskaya, Avital Oliver, Marvin Ritter, Bertrand Rondepierre, Andreas Steiner, and Marc van Zee. Flax: A neural network library and ecosystem for JAX, 2024. URL <http://github.com/google/flax>.
- Dan Hendrycks and Kevin Gimpel. Gaussian error linear units (gelus). *arXiv preprint arXiv:1606.08415*, 2016.
- Irina Higgins, Loic Matthey, Arka Pal, Christopher Burgess, Xavier Glorot, Matthew Botvinick, Shakir Mohamed, and Alexander Lerchner. beta-VAE: Learning basic visual concepts with a constrained variational framework. In *International Conference on Learning Representations*, 2017a.
- Irina Higgins, Arka Pal, Andrei Rusu, Loic Matthey, Christopher Burgess, Alexander Pritzel, Matthew Botvinick, Charles Blundell, and Alexander Lerchner. Darla: Improving zero-shot transfer in reinforcement learning. In *International Conference on Machine Learning*, pp. 1480–1490. PMLR, 2017b.
- Kyle Hsu, William Dorrell, James Whittington, Jiajun Wu, and Chelsea Finn. Disentanglement via latent quantization. *Advances in Neural Information Processing Systems*, 36, 2024a.
- Kyle Hsu, Jubayer Ibn Hamid, Kaylee Burns, Chelsea Finn, and Jiajun Wu. Tripod: Three complementary inductive biases for disentangled representation learning. In *International Conference on Machine Learning*, pp. 19101–19122. PMLR, 2024b.

- Jiaheng Hu, Zizhao Wang, Peter Stone, and Roberto Martín-Martín. Disentangled unsupervised skill discovery for efficient hierarchical reinforcement learning. *Advances in Neural Information Processing Systems*, 37:76529–76552, 2024.
- Aapo Hyvärinen and Hiroshi Morioka. Unsupervised feature extraction by time-contrastive learning and nonlinear ica. *Advances in neural information processing systems*, 29, 2016.
- Aapo Hyvärinen, Ilyes Khemakhem, and Hiroshi Morioka. Nonlinear independent component analysis for principled disentanglement in unsupervised deep learning. *Patterns*, 4(10), 2023.
- Aapo Hyvärinen, Hiroaki Sasaki, and Richard Turner. Nonlinear ica using auxiliary variables and generalized contrastive learning. In *The 22nd International Conference on Artificial Intelligence and Statistics*, pp. 859–868. PMLR, 2019.
- Nan Rosemary Ke, Aniket Rajiv Didolkar, Sarthak Mittal, Anirudh Goyal, Guillaume Lajoie, Stefan Bauer, Danilo Jimenez Rezende, Yoshua Bengio, Christopher Pal, and Michael Curtis Mozer. Systematic evaluation of causal discovery in visual model based reinforcement learning. In *Thirty-fifth Conference on Neural Information Processing Systems Datasets and Benchmarks Track (Round 2)*.
- Michael Kearns and Daphne Koller. Efficient reinforcement learning in factored mdps. In *Proceedings of the 16th international joint conference on Artificial intelligence-Volume 2*, pp. 740–747, 1999.
- Michael Kearns and Satinder Singh. Near-optimal reinforcement learning in polynomial time. *Machine learning*, 49:209–232, 2002.
- Ilyes Khemakhem, Diederik Kingma, Ricardo Monti, and Aapo Hyvärinen. Variational autoencoders and nonlinear ica: A unifying framework. In *International Conference on Artificial Intelligence and Statistics*, pp. 2207–2217. PMLR, 2020a.
- Ilyes Khemakhem, Ricardo Monti, Diederik Kingma, and Aapo Hyvärinen. Ice-beem: Identifiable conditional energy-based deep models based on nonlinear ica. *Advances in Neural Information Processing Systems*, 33:12768–12778, 2020b.
- Hyunjik Kim and Andriy Mnih. Disentangling by factorising. In *International conference on machine learning*, pp. 2649–2658. PMLR, 2018.
- Diederik P. Kingma and Max Welling. Auto-encoding variational bayes. In Yoshua Bengio and Yann LeCun (eds.), *2nd International Conference on Learning Representations, ICLR 2014, Banff, AB, Canada, April 14-16, 2014, Conference Track Proceedings*, 2014.
- David A Klindt, Lukas Schott, Yash Sharma, Ivan Ustyuzhaninov, Wieland Brendel, Matthias Bethge, and Dylan Paiton. Towards nonlinear disentanglement in natural data with temporal sparse coding. In *International Conference on Learning Representations*, 2020.
- Daphne Koller and Ronald Parr. Policy iteration for factored mdps. In *Proceedings of the Sixteenth conference on Uncertainty in artificial intelligence*, pp. 326–334, 2000.
- Harold W Kuhn. The hungarian method for the assignment problem. *Naval research logistics quarterly*, 2(1-2):83–97, 1955.
- Sébastien Lachapelle, Pau Rodriguez, Yash Sharma, Katie E Everett, Rémi Le Priol, Alexandre Lacoste, and Simon Lacoste-Julien. Disentanglement via mechanism sparsity regularization: A new principle for nonlinear ica. In *Conference on Causal Learning and Reasoning*, pp. 428–484. PMLR, 2022.
- Sébastien Lachapelle, Pau Rodríguez López, Yash Sharma, Katie Everett, Rémi Le Priol, Alexandre Lacoste, and Simon Lacoste-Julien. Nonparametric partial disentanglement via mechanism sparsity: Sparse actions, interventions and sparse temporal dependencies. *arXiv preprint arXiv:2401.04890*, 2024.
- Anson Lei, Bernhard Schölkopf, and Ingmar Posner. Variational causal dynamics: Discovering modular world models from interventions. *arXiv preprint arXiv:2206.11131*, 2022.

- Sergey Levine, Chelsea Finn, Trevor Darrell, and Pieter Abbeel. End-to-end training of deep visuomotor policies. *Journal of Machine Learning Research*, 17(39):1–40, 2016. URL <http://jmlr.org/papers/v17/15-522.html>.
- Timothy P Lillicrap, Jonathan J Hunt, Alexander Pritzel, Nicolas Heess, Tom Erez, Yuval Tassa, David Silver, and Daan Wierstra. Continuous control with deep reinforcement learning. *4th International Conference on Learning Representations*, 2016.
- Phillip Lippe, Sara Magliacane, Sindy Löwe, Yuki M Asano, Taco Cohen, and Stratis Gavves. Citris: Causal identifiability from temporal intervened sequences. In *International Conference on Machine Learning*, pp. 13557–13603. PMLR, 2022.
- Phillip Lippe, Sara Magliacane, Sindy Löwe, Yuki M Asano, Taco Cohen, and Efstratios Gavves. Biscuit: Causal representation learning from binary interactions. In *Uncertainty in Artificial Intelligence*, pp. 1263–1273. PMLR, 2023a.
- Phillip Lippe, Sara Magliacane, Sindy Löwe, Yuki M Asano, Taco Cohen, and Efstratios Gavves. Causal representation learning for instantaneous and temporal effects in interactive systems. In *The Eleventh International Conference on Learning Representations*, 2023b.
- Yuren Liu, Biwei Huang, Zhengmao Zhu, Honglong Tian, Mingming Gong, Yang Yu, and Kun Zhang. Learning world models with identifiable factorization. *Advances in Neural Information Processing Systems*, 36:31831–31864, 2023.
- Francesco Locatello, Stefan Bauer, Mario Lucic, Gunnar Raetsch, Sylvain Gelly, Bernhard Schölkopf, and Olivier Bachem. Challenging common assumptions in the unsupervised learning of disentangled representations. In *international conference on machine learning*, pp. 4114–4124. PMLR, 2019.
- Francesco Locatello, Ben Poole, Gunnar Rätsch, Bernhard Schölkopf, Olivier Bachem, and Michael Tschannen. Weakly-supervised disentanglement without compromises. In *International conference on machine learning*, pp. 6348–6359. PMLR, 2020.
- Ilya Loshchilov and Frank Hutter. Decoupled weight decay regularization. In *International Conference on Learning Representations*, 2019. URL <https://openreview.net/forum?id=Bkg6RiCqY7>.
- Dipendra Misra, Qinghua Liu, Chi Jin, and John Langford. Provable rich observation reinforcement learning with combinatorial latent states. In *International Conference on Learning Representations*, 2021.
- Volodymyr Mnih, Koray Kavukcuoglu, David Silver, Andrei A Rusu, Joel Veness, Marc G Bellemare, Alex Graves, Martin Riedmiller, Andreas K Fidjeland, Georg Ostrovski, et al. Human-level control through deep reinforcement learning. *nature*, 518(7540):529–533, 2015.
- Aaron van den Oord, Yazhe Li, and Oriol Vinyals. Representation learning with contrastive predictive coding. *arXiv preprint arXiv:1807.03748*, 2018.
- Ian Osband and Benjamin Van Roy. Near-optimal reinforcement learning in factored mdps. *Advances in Neural Information Processing Systems*, 27, 2014.
- Eduardo Pignatelli, Jarek Liesen, Robert Tjarko Lange, Chris Lu, Pablo Samuel Castro, and Laura Toni. Navix: Scaling minigrid environments with jax. *arXiv preprint arXiv:2407.19396*, 2024.
- Silviu Pitisi, Elliot Creager, and Animesh Garg. Counterfactual data augmentation using locally factored dynamics. *Advances in Neural Information Processing Systems*, 33:3976–3990, 2020.
- Silviu Pitisi, Elliot Creager, Ajay Mandlekar, and Animesh Garg. Mocoda: Model-based counterfactual data augmentation. *Advances in Neural Information Processing Systems*, 35:18143–18156, 2022.
- Martin L. Puterman. *Markov Decision Processes: Discrete Stochastic Dynamic Programming*. Wiley Series in Probability and Statistics. Wiley, 1994. ISBN 978-0-47161977-2. doi: 10.1002/9780470316887.

- Rafael Rodriguez-Sanchez and George Konidaris. Learning abstract world models for value-preserving planning with options. *Reinforcement Learning Journal*, 4:1733–1758, 2024.
- Jürgen Schmidhuber. Learning factorial codes by predictability minimization. *Neural computation*, 4(6):863–879, 1992.
- Bernhard Schölkopf, Francesco Locatello, Stefan Bauer, Nan Rosemary Ke, Nal Kalchbrenner, Anirudh Goyal, and Yoshua Bengio. Toward causal representation learning. *Proceedings of the IEEE*, 109(5):612–634, 2021.
- Julian Schrittwieser, Ioannis Antonoglou, Thomas Hubert, Karen Simonyan, Laurent Sifre, Simon Schmitt, Arthur Guez, Edward Lockhart, Demis Hassabis, Thore Graepel, et al. Mastering atari, go, chess and shogi by planning with a learned model. *Nature*, 588(7839):604–609, 2020.
- Maximilian Seitzer, Bernhard Schölkopf, and Georg Martius. Causal influence detection for improving efficiency in reinforcement learning. *Advances in Neural Information Processing Systems*, 34:22905–22918, 2021.
- Chandler Squires, Anna Seigal, Salil S Bhate, and Caroline Uhler. Linear causal disentanglement via interventions. In *International conference on machine learning*, pp. 32540–32560. PMLR, 2023.
- Alexander L. Strehl, Carlos Diuk, and Michael L. Littman. Efficient structure learning in factored-state mdps. In *Proceedings of the 22nd National Conference on Artificial Intelligence - Volume 1*, AAAI’07, pp. 645–650. AAAI Press, 2007. ISBN 9781577353232.
- Richard S Sutton, Doina Precup, and Satinder Singh. Between mdps and semi-mdps: A framework for temporal abstraction in reinforcement learning. *Artificial intelligence*, 112(1-2):181–211, 1999.
- Valentin Thomas, Emmanuel Bengio, William Fedus, Jules Pondard, Philippe Beaudoin, Hugo Larochelle, Joelle Pineau, Doina Precup, and Yoshua Bengio. Disentangling the independently controllable factors of variation by interacting with the world. *arXiv preprint arXiv:1802.09484*, 2018.
- Yi Tian, Jian Qian, and Suvrit Sra. Towards minimax optimal reinforcement learning in factored markov decision processes. *Advances in Neural Information Processing Systems*, 33:19896–19907, 2020.
- Burak Varici, Emre Acartürk, Karthikeyan Shanmugam, and Ali Tajer. General identifiability and achievability for causal representation learning. In *International Conference on Artificial Intelligence and Statistics*, pp. 2314–2322. PMLR, 2024.
- Christopher M Vigorito and Andrew G Barto. Incremental structure learning in factored mdps with continuous states and actions. *University of Massachusetts Amherst-Department of Computer Science, Tech. Rep*, 2009.
- Christopher M. Vigorito and Andrew G. Barto. Intrinsically motivated hierarchical skill learning in structured environments. *IEEE Transactions on Autonomous Mental Development*, 2(2):132–143, 2010. doi: 10.1109/TAMD.2010.2050205.
- Julius von Kügelgen, Michel Besserve, Liang Wendong, Luigi Gresele, Armin Kekić, Elias Bareinboim, David Blei, and Bernhard Schölkopf. Nonparametric identifiability of causal representations from unknown interventions. *Advances in Neural Information Processing Systems*, 36, 2024.
- Tongzhou Wang, Simon S Du, Antonio Torralba, Phillip Isola, Amy Zhang, and Yuandong Tian. De-noised mdps: Learning world models better than the world itself. *arXiv preprint arXiv:2206.15477*, 2022a.
- Zizhao Wang, Xuesu Xiao, Zifan Xu, Yuke Zhu, and Peter Stone. Causal dynamics learning for task-independent state abstraction. In Kamalika Chaudhuri, Stefanie Jegelka, Le Song, Csaba Szepesvari, Gang Niu, and Sivan Sabato (eds.), *Proceedings of the 39th International Conference on Machine Learning*, volume 162 of *Proceedings of Machine Learning Research*, pp. 23151–23180. PMLR, 17–23 Jul 2022b.

- Zizhao Wang, Jiaheng Hu, Peter Stone, and Roberto Martín-Martín. Elden: Exploration via local dependencies. *Advances in Neural Information Processing Systems*, 36:15456–15474, 2023.
- Zizhao Wang, Jiaheng Hu, Caleb Chuck, Stephen Chen, Roberto Martín-Martín, Amy Zhang, Scott Niekum, and Peter Stone. Skild: Unsupervised skill discovery guided by factor interactions. In Amir Globersons, Lester Mackey, Danielle Belgrave, Angela Fan, Ulrich Paquet, Jakub M. Tomczak, and Cheng Zhang (eds.), *Advances in Neural Information Processing Systems 38: Annual Conference on Neural Information Processing Systems 2024, NeurIPS 2024, Vancouver, BC, Canada, December 10 - 15, 2024*, 2024.
- Ziping Xu and Ambuj Tewari. Near-optimal reinforcement learning in factored mdps: Oracle-efficient algorithms for the non-episodic setting. *Advances in Neural Information Processing Systems*, 33, 2020.
- Jiaqi Zhang, Kristjan Greenewald, Chandler Squires, Akash Srivastava, Karthikeyan Shanmugam, and Caroline Uhler. Identifiability guarantees for causal disentanglement from soft interventions. *Advances in Neural Information Processing Systems*, 36:50254–50292, 2023.

A Theoretical Results

Definition A.1 (Identifiability). An encoder $f : X \rightarrow Z$ identifies \mathcal{S} if there exists a permutation π and functions $h_i : \mathcal{S}_i \rightarrow Z_{\pi(i)}$ that are diffeomorphism such that $s_i = h(z_{\pi(i)})$. That is, each latent factor learned is equivalent to a ground truth factor up to a permutation.

Lemma A.2 (Local Identifiability of the Independently Controllable Factors). *Let the learned encoder $f : X \rightarrow Z$ be a diffeomorphism. If the following conditions hold*

1. *The action effects are **sufficiently different** from the natural dynamics. That is, there exists $i \in [K]$*

$$\frac{\partial}{\partial s'_i} \frac{T_i(s'_i | s, a)}{T(s'_i | s, a_0)} \neq 0$$

for $s \in \tilde{\mathcal{S}} \subseteq \mathcal{S}$, almost surely. Moreover, there exists at least an action that affects each s_i (independently controllability)

2. *All energy function approximate the factor forward dynamics $E(z'_i, a, z) \propto \log T(z'_i | z, a)$;*
3. **(Sparsity)** *The learned score differences*

$$\frac{\partial}{\partial z'_i} \Delta E_i^a = \frac{\partial}{\partial z'_i} [E(z'_i, a, z) - E(z'_i, a_0, z)] \neq 0$$

for at most one variable j .

then, there exists a factor-wise diffeomorphism $h : \mathcal{S} \rightarrow Z$ between the learned encoding Z and the underlying ground truth factors of variation \mathcal{S} .

Proof. Let h be a diffeomorphism between \mathcal{S} and Z . Given that the ground truth observation function is a diffeomorphism $o : \mathcal{S} \rightarrow X$ and, by assumption, the learned encoding is also a diffeomorphism. We can see that $h(s) = f(o(s))$. We need to prove that there exists a permutation $\pi : [K] \rightarrow [K]$ such that the permuted Jacobian of h , $P_\pi J_h$, is a diagonal matrix.

Given that h is a diffeomorphism, J_h exists.

Moreover, for each binary classifier, we know that at an optimum they converge to:

$$\log \frac{T(s' | s, a_n)}{T(s' | s, a_0)} = \sum_{l=1}^K E(z'_l, a_n, z) - E(z'_l, a_0, z) + C(z, a_n) \quad \forall a_n \in A \setminus \{a_0\}; \quad (7)$$

where $C(z, a)$ is a constant resulting from the normalization constants that are not estimated in ACF. By taking the gradient with respect to s' using the chain rule, we get that

$$\nabla_{s'} \log \frac{T(s' | s, a_n)}{T(s' | s, a_0)} = \sum_{l=1}^K J_h^T(s') \nabla_{z'} [E(z'_l, a_n, z) - E(z'_l, a_0, z)] \quad \forall a_n \in A \setminus \{a_0\} \quad (8)$$

Let $\rho(a_i) \mapsto [K]$ be the maps each action to its affected factor. Hence, by considering our sparse interaction model in Equation 1 we get that each classifier is a function of the variables affected by a_n . That is,

$$\begin{aligned} \nabla_{s'} \log \frac{T(s'_{\rho(a_n)} | s, a_n)}{T(s'_{\rho(a_n)} | s, a_0)} &= \sum_{l=1}^K J_h^T(s') \nabla_{z'} [E(z'_l, a_n, z) - E(z'_l, a_0, z)] \quad \forall a_n \in A \setminus \{a_0\} \quad (9) \\ &= J_h^T \begin{bmatrix} \frac{\partial}{\partial z'_1} (E(z'_1, a_n, z) - E(z'_1, a_0, z)) \\ \vdots \\ \frac{\partial}{\partial z'_K} (E(z'_K, a_n, z) - E(z'_K, a_0, z)) \end{bmatrix} \end{aligned} \quad (10)$$

Moreover, consider a set of the actions $\bar{\mathcal{A}} \subseteq \mathcal{A} \setminus \{a_0\}$ such that each action affects one of the ground truth variables, that is, they are independently controllable.

We can write the above conditions in matrix form by stacking the gradients of all the actions in $\bar{\mathcal{A}}$.

Let $\Delta S(z' | z)$ be the matrices of learned score differences

$$[\Delta S(z' | z)]_{l,n} = \frac{\partial}{\partial z'_l} [E(z'_l, a_n, z) - E(z'_l, a_0, z)]; \quad (11)$$

and $\Delta S(s' | s)$ be the matrices of score differences in s' .

$$[\Delta S(s' | s)]_{i,n} = \begin{cases} \frac{\partial}{\partial s'_i} \log \frac{T(s'_i | s, a_n)}{T(s'_i | s, a_0)} & \text{if } i = \rho(a_n) \\ 0 & \text{otherwise} \end{cases} \quad (12)$$

Hence, we can rewrite Equation 8 as

$$\Delta S(s' | s) = J_h^T(s') \Delta S(z' | z). \quad (13)$$

There exists s such that all columns of $\Delta S(s' | s)$ has only one element different from zero and it is full rank because each factor is affected by at least one action. Moreover, given $J_h(s')$ is full rank because is a diffeomorphism and $\Delta S(z' | z)$ must also have exactly one element different from zero (sparsity condition).

Thus, $J_h(s')$ must have only one element different from zero per row. To see this, consider the j th column of $\Delta S(z' | z)_j = \beta e_r$ where $\beta \in \mathbb{R}$ and r is the row different from zero. Hence,

$$\begin{aligned} \Delta S(s' | s)_j &= J_h^T(s') \Delta S(z' | z)_j; \\ &= \beta J_h^T(s') e_r; \\ &= \beta J_h^T(s')_{:,r}; \end{aligned}$$

and, therefore, $J_h(s')_r$ the r th column of the Jacobian must have one element different from zero. Therefore, $J_h(s')$ must be 1-sparse.

Finally, there exists a permutation $P(s')$ such that $J_h(s') = P(s')D(s')$ where $D(s')$ is a diagonal matrix. That is, there exists h that is a factorwise transformation of s up to a permutation.

□

This lemma shows that there exists a permutation in s where action can have independent control over the factors. However, this does not guarantee the encoding is consistent because the permutation could be different in other parts of the space.

The following proposition establishes some conditions that guarantee identifiability globally.

Proposition A.3 (Global Identifiability of Independently Controllable Factors). *Let the local conditions for identifiability hold. Moreover, assume that $\mathcal{S} \subset \mathbb{R}^K$ is connected. Then there exists a unique permutation π for all $s \in \mathcal{S}$.*

Proof. Let $s_0 \in \mathcal{S}$ be a fix point. We know that the Jacobian $J_h(s_0) = P_\pi(s_0)D(s_0)$ because of local identifiability. Let π_{s_0} be the permutation corresponding to the matrix $P_\pi(s_0)$.

Moreover, because h is a diffeomorphism, we have that each derivative $h'_i(s)$ is continuous and non-vanishing.

Therefore, there exists a neighborhood U such that $h_{\pi_{s_0}(i)}(s_{\pi_{s_0}(i)}) \neq 0$ for all $s \in U$.

Because of continuity of J_h , we must have that per each row it's nonzero element remains so and, similarly, for the zero elements of the row. Therefore, the permutation $\pi_{s_0} = \pi_s$ for all $s \in U$. This makes the permutation locally constant.

Finally, because there’s a finite discrete number of permutations and \mathcal{S} is connected, it implies that $\pi_s = \pi$ globally constant in \mathcal{S} .

□

B Extended Empirical Results

Anonymized code at https://anonymous.4open.science/r/factored_rl-EE0A.

B.1 Network Architectures

All networks were implemented using JAX (Bradbury et al., 2018) and Flax NNX (Heek et al., 2024).

Table 2: All methods use the same Residual Convolutional architecture for encoder (and decoder, when required). All MLPs use SiLU activations. Latent encodings are Tanh to keep between $(-1, 1)$ except for DMS.

Component	DoorKey(8x8)	Taxi	Grid2D	FourRooms
latent_dim (d)	7	6	2	5
n_actions n_a	10	6	5	10
ACF Energy[$\times d$]	$(d + n_a) \rightarrow 256 \rightarrow n_a$			
ACF Inverse	$2d \rightarrow 128 \rightarrow n_a$			
ACF Policy	$d \rightarrow 256 \rightarrow 256 \rightarrow n_a$			
GCL Energy[$\times d$]	$(d + n_a) \rightarrow 128 \rightarrow 128 \rightarrow n_a$			
DMS Transition[$\times d$]	$(d + n_a) \rightarrow 256 \rightarrow 1$			
Markov Inverse	$2d \rightarrow 128 \rightarrow n_a$			
Markov Ratio	$2d \rightarrow 128 \rightarrow 1$			

Pixel-level Encoder & Decoder.

We parameterize the residual blocks by doubling the depth of the output feature map until reaching a minimum resolution (`min_res`) (4 for all our experiments) starting from a minimum depth (24 for all our experiments). This is similar to the residual CNN used in Hafner et al. (2025). Table 2 show the details of the MLPs used.

- **Residual Encoder:**
 - Positional Embeddings (x, y channels).
 - Cascade of downsampling ResidualBlocks: stride-2 3×3 convolution \rightarrow RMSNorm \rightarrow SiLU, plus two 1×1 conv residual layers.
 - Flatten \rightarrow 2-layer MLP ($256 \rightarrow 256$, SiLU, then Tanh) \rightarrow latent_dim(d)
- **Residual Decoder:**
 - MLP up-projection from latent_dim \rightarrow min_res \times min_res \times D .
 - Stack of transposed ResidualBlocks (stride-2 conv^T, RMSNorm, SiLU, ...)
 - Central crop to $32 \times 32 \rightarrow$ Tanh activation.
- **MLPs** All MLPs have SiLU activations (Hendrycks & Gimpel, 2016).

B.2 Domains

Grid2D

Actions No-op, Up, Down, Left, Right;

State Space Continuous 2D space

Observations $32 \times 32 \times 3$ pixel rendering.

Taxi implementation in JAX.

Actions No-op, Up, Down, Left, Right;

State Space 5×5 , 1 passenger, 4 different goals positions;

Observations 32×32 RGB rendering.

Minigrid-FourRooms & Minigrid-DoorKey(8x8)

Actions No-op, Rotate clockwise, Rotate counterclockwise, Forward, Backward, Right, Left, Pickup, Open, Done;

State Space 16×16 grid (position) and orientation (North, South, East, West);

Observation RGB 32×32 rendering.

B.3 Hyperparameters, Tuning and Computational Resources

We tune the hyperparameters by random search allocating 50 samples to each method and each configuration run with 5 different seeds. Tables 3, 4, 5, and 6 show the details for the best results for all methods and domains. Each trial was run in a NVIDIA GeForce RTX3090 24GB. Each trial took 15min. All experiments used 150K transitions.

Table 3: Hyperparameters and coefficient weights for the ACF baseline across four domains.

Hyperparameter	DoorKey-Uniform	Taxi	Grid2D	FourRooms
<i>Training</i>				
batch_size	128	128	128	128
lr	4.0966×10^{-4}	2.9126×10^{-4}	2.27497×10^{-4}	3.6392×10^{-4}
epochs	100	200	200	200
<i>ACF Coefficients</i>				
λ_{fwd}	97.815	31.444	95.395	40.736
λ_r	25.623	5.018	48.560	16.963
λ_{inv}	22.094	1.000	1.000	97.365
λ_π	1.610	9.916	1.332	22.764

Table 4: Hyperparameters and coefficient weights for the GCL baseline across domains.

Hyperparameter	DoorKey(8x8)	Taxi	Grid2D	FourRooms
<i>Training</i>				
batch_size	128	128	128	128
lr	2.0363×10^{-4}	4.4530×10^{-4}	1.6031×10^{-4}	2.7661×10^{-5}
epochs	100	200	200	200
<i>GCL Coefficients</i>				
classifier_coeff	60.444	27.293	90.737	51.030
recons_coeff	9.26×10^{-8}	4.53×10^{-10}	0.193	3.50×10^{-4}

B.4 Detailed Empirical Results

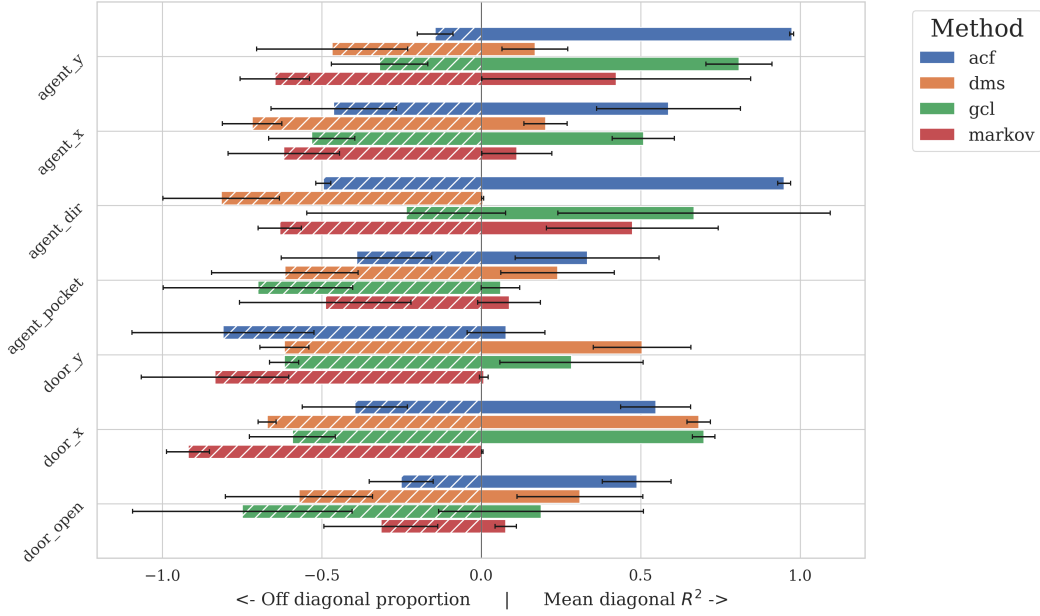
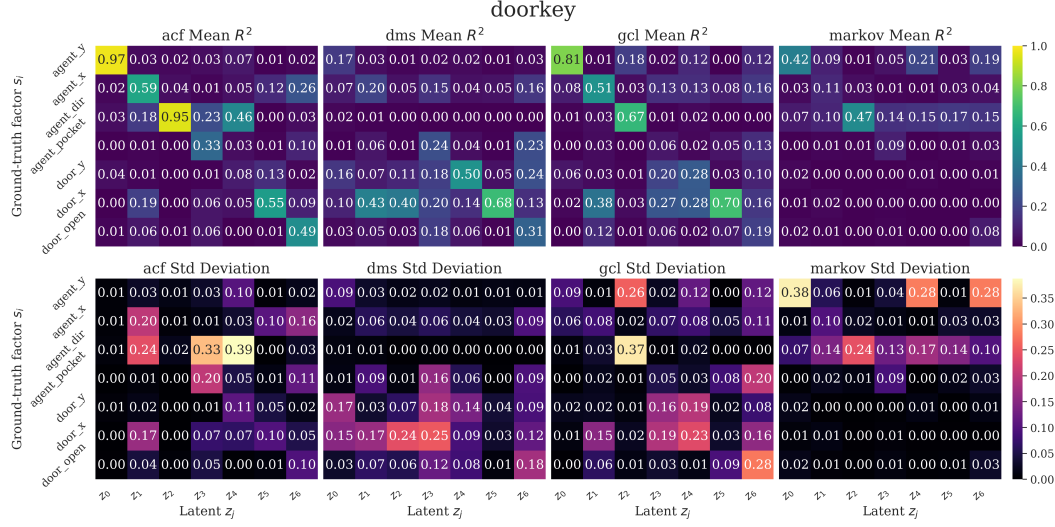
Detailed results for DoorKey (Figure ??), Minigrid-FourRooms (Figure 6), Taxi (Figure 7b), and Grid2D (Figure 8).

Table 5: Hyperparameters and coefficient weights for the DMS baseline across domains.

Hyperparameter / Coefficient	DoorKey(8×8)	Taxi	Grid2D	FourRooms
<i>Training</i>				
batch_size	128	128	128	128
lr	3.5332×10^{-4}	9.6832×10^{-5}	7.5007×10^{-5}	4.0218×10^{-4}
epochs	100	200	200	200
<i>DMS Coefficients</i>				
elbo_const	4.737	67.349	42.948	5.225
action_sparsity_const	3.536	36.881	91.982	9.878
state_sparsity_const	2.557	8.024	1.000	6.091
gumbel_temp	7.417	1.000	6.360	3.465
l2_reg_const	0.0015	0.0023	0.2805	0.0060

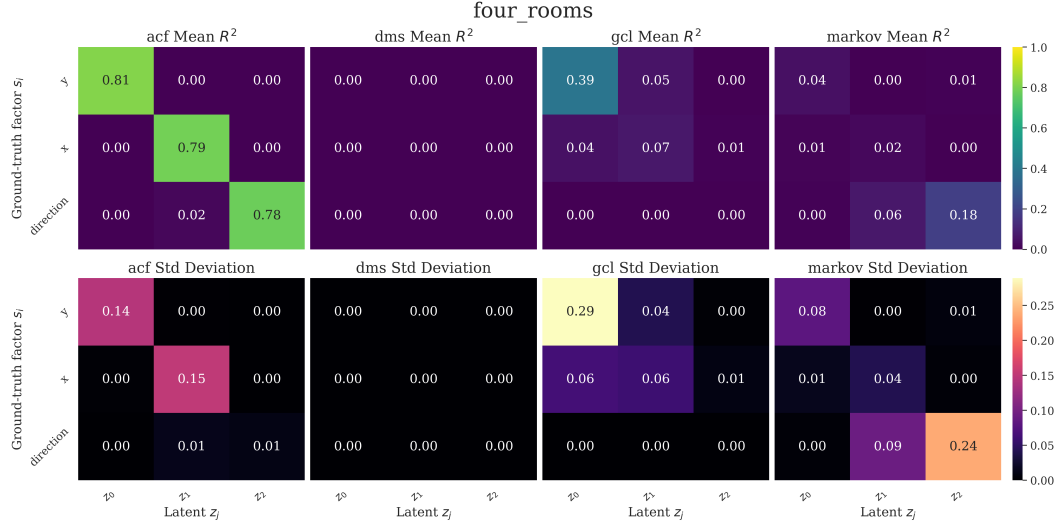
Table 6: Hyperparameters and coefficient weights for the Markov baseline across domains.

Hyperparameter / Coefficient	DoorKey(8×8)	Taxi	Grid2D	FourRooms
<i>Training</i>				
batch_size	128	128	128	128
lr	4.5536×10^{-4}	3.9622×10^{-4}	4.2654×10^{-4}	1.5854×10^{-4}
epochs	100	200	200	200
<i>Markov Coefficients</i>				
inverse_const	6.009	66.916	78.480	9.472
ratio_const	8.519	42.518	1.000	0.311
smoothness_const	2.092	8.234	84.905	9.691

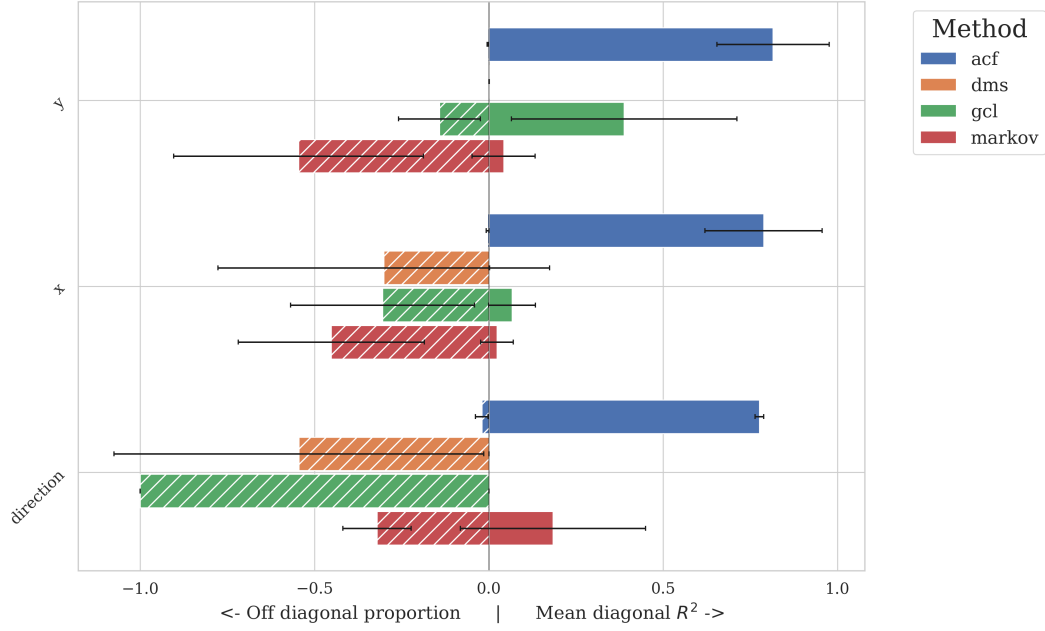


(b) Off diagonal proportion vs. Mean diagonal value per state

Figure 5: **DoorKey** Factorization Results



(a) R^2 matrices for **Minigrid-FourRooms** for 5 seeds: [Top] Mean R^2 matrices. [Bottom] Standard Deviation



(b) Off diagonal proportion vs. Mean diagonal value per state

Figure 6: **Minigrid-FourRooms** Factorization Results

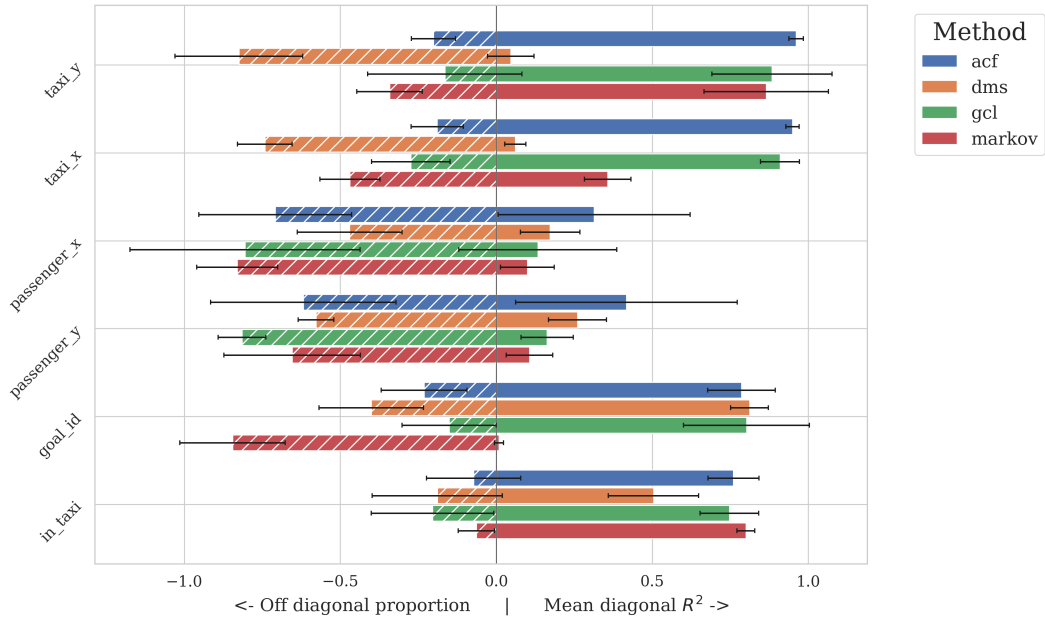
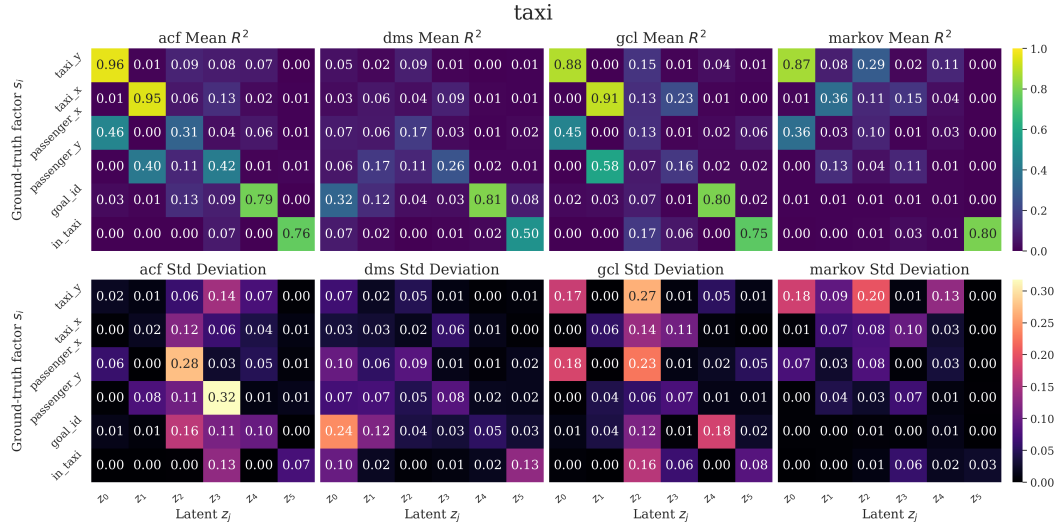
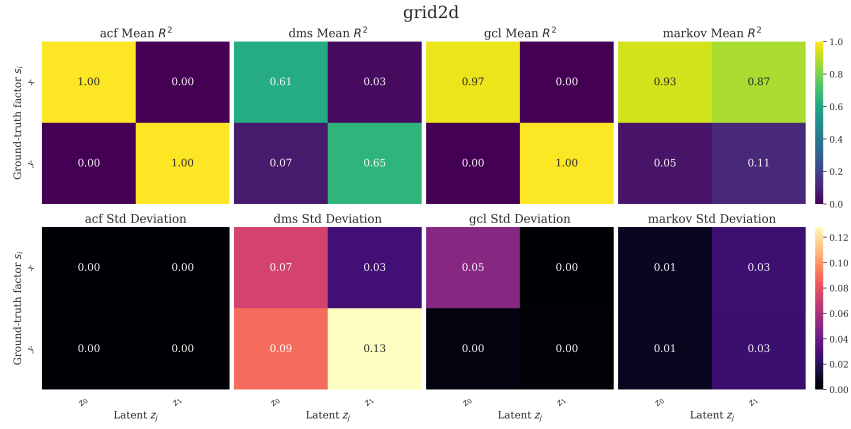
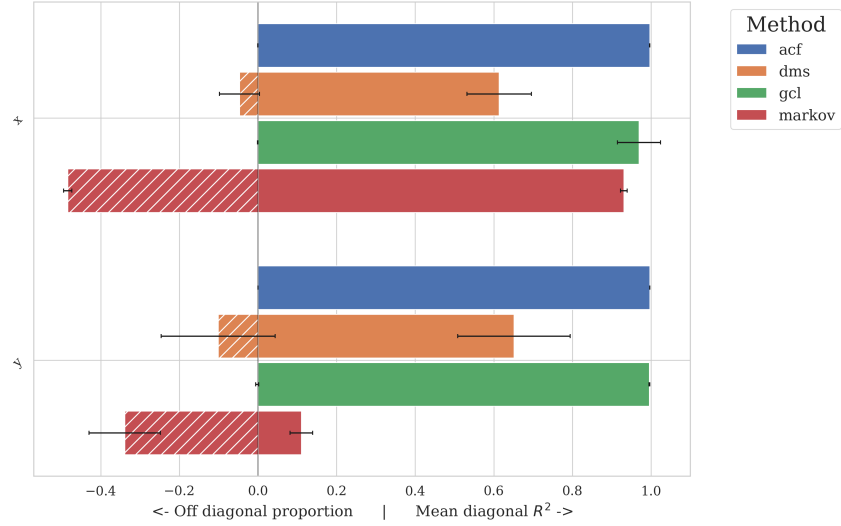


Figure 7: **Taxi** Factorization Results



(a) R^2 matrices for **Grid2D** for 5 seeds: [Top] Mean R^2 matrices. [Bottom] Standard Deviation



(b) Off diagonal proportion vs. Mean diagonal value per state

Figure 8: **Grid2D** Factorization Results